

High Efficient and Stable Thiol-Modified Dendritic Mesoporous Silica Nanospheres Supported Gold catalysts for Gas-phase Selective Oxidation of Benzyl Alcohol with Ultra-Long Lifetime

Liu-Xi Zheng, Bo-Peng, Kun Zhang**

Shanghai Key Laboratory of Green Chemistry and Chemical Processes, College of Chemistry and Molecular Engineering, East China Normal University, Shanghai 200062, China; (Liu-Xi Zheng, Bo-Peng, Jia-Feng Zhou, Bing-Qian Shan, Qing-Song Xue, Kun Zhang)

Laboratoire de chimie, Ecole Normale Supérieure de Lyon, Institut de Chimie de Lyon, Université de Lyon, 46 Allée d'Italie, 69364 Lyon cedex 07, France; (Kun Zhang)

Shandong Provincial Key Laboratory of Chemical Energy Storage and Novel Cell Technology, School of Chemistry and Chemical Engineering, Liaocheng University, Liaocheng 252059, Shandong, P. R. China. (Kun Zhang)

*Corresponding author, Email: xiaogen_ban@sina.com (Bo-Peng); kzhang@chem.ecnu.edu.cn (Kun Zhang)

ABSTRACT: Thiol-modified dendritic mesoporous silica nanospheres (DMSNs) supported Au catalyst were facilely prepared and used in gas-phase selective oxidation of benzyl alcohol with O₂ as the oxidant. The Au/DMSNs-4.4%SH catalyst with low loading of Au (~2%) and proper amount of thiol ligand (~4.4%) achieved high conversion of benzyl alcohol (*Conv.* 91%) and selectivity for benzaldehyde (*Sel.* 98%) and unprecedented lifetime up to 820 h at 250 °C. The dramatically increased lifetime is the consequence of the strong stabilization of active gold nanoparticles by thiol ligand and the effective mass diffusion of DMSNs with opened three-dimensional mesoporous networks.

1. INTRODUCTION:

Selective oxidation of alcohols to aldehydes, especially benzyl alcohol-to-benzaldehyde, is one of the pivotal reaction in organic synthesis and is of particular importance in both fundamental academic research and practical industrial applications.¹⁻⁵ However, most of the classic transformations usually require stoichiometric amounts of high-valent metal salts oxidants or organic compounds as the oxidants, which are expensive and have serious toxicity issues associated with them.⁶ Over the past two decades, lots of supported metal (such as Cu, Ag and Au, *etc.*) catalysts have been developed for the gas-phase oxidation of benzyl alcohol⁶⁻¹⁶. Nevertheless, most of these catalysts were used at relatively high reaction temperature (generally over 300 °C) and showed a poor stability in gas-phase oxidation of benzyl alcohol. Recently, ordered nanoporous silica FDU-12 with ultra-large pores supported Au nanoparticles (NPs) catalyst exhibited excellent stability (~ 450 h) in gas-phase selective oxidation of benzyl alcohol at 250 °C.¹⁷ The large and open porous network was thought to be beneficial to mass diffusion and thus suppressed coke deposition on Au NPs.

DMSNs with centre-radial oriented open and large mesopores can provide greater pore accessibility and faster molecular diffusion, and can be easily functionalized for subsequently doping of active sites, thus it could be an ideal platform for the preparation of highly efficient heterogeneous nanocatalyst, especially for high temperature catalytic reaction.¹⁸⁻²⁵ Herein, Au NPs catalysts supported on thiol-modified DMSNs (Au/DMSNs-x%SH, in which x represented the weight loss of grafted thiol ligands as reference to non-modified DMSNs calculated in TG analysis) were prepared and tested in the gas-phase selective oxidation of benzyl alcohol, it demonstrated that the catalytic performance was highly related to the content of grafted thiol group. The Au/DMSNs-4.4%SH catalyst exhibited the best catalytic performance at low reaction temperature of 250 °C, achieving a benzyl alcohol conversion of 91% and benzaldehyde selectivity of 98% with long lifetime up to 820 hours beyond the previously reported Au-based catalysts. The high catalytic performance of our Au/DMSNs-4.4%SH catalysts is contributed to the unique dendritic nanostructure of DMSNs and the strong S-Au binding energy combined to improve the dispersibility and high-temperature anti-sintering of Au NPs.

2. RESULTS AND DISCUSSION

DMSNs modified with different content of thiol ligands (3.4%, 4.4%, and 6.0%, Fig. 1a) can be readily prepared by post-grafting technique with (3-mercaptopropyl) trimethoxysilane (MPTMS) as organosilane coupling agents in the presence of propylamine (PA) as a base catalyst (synthetic details in supporting information), wherein the addition of PA significantly improves the grafting efficiency of thiol groups on the silica pore frameworks. The obtained samples were denoted as DMSNs-x%SH, in which x represented the weight loss of grafted thiol

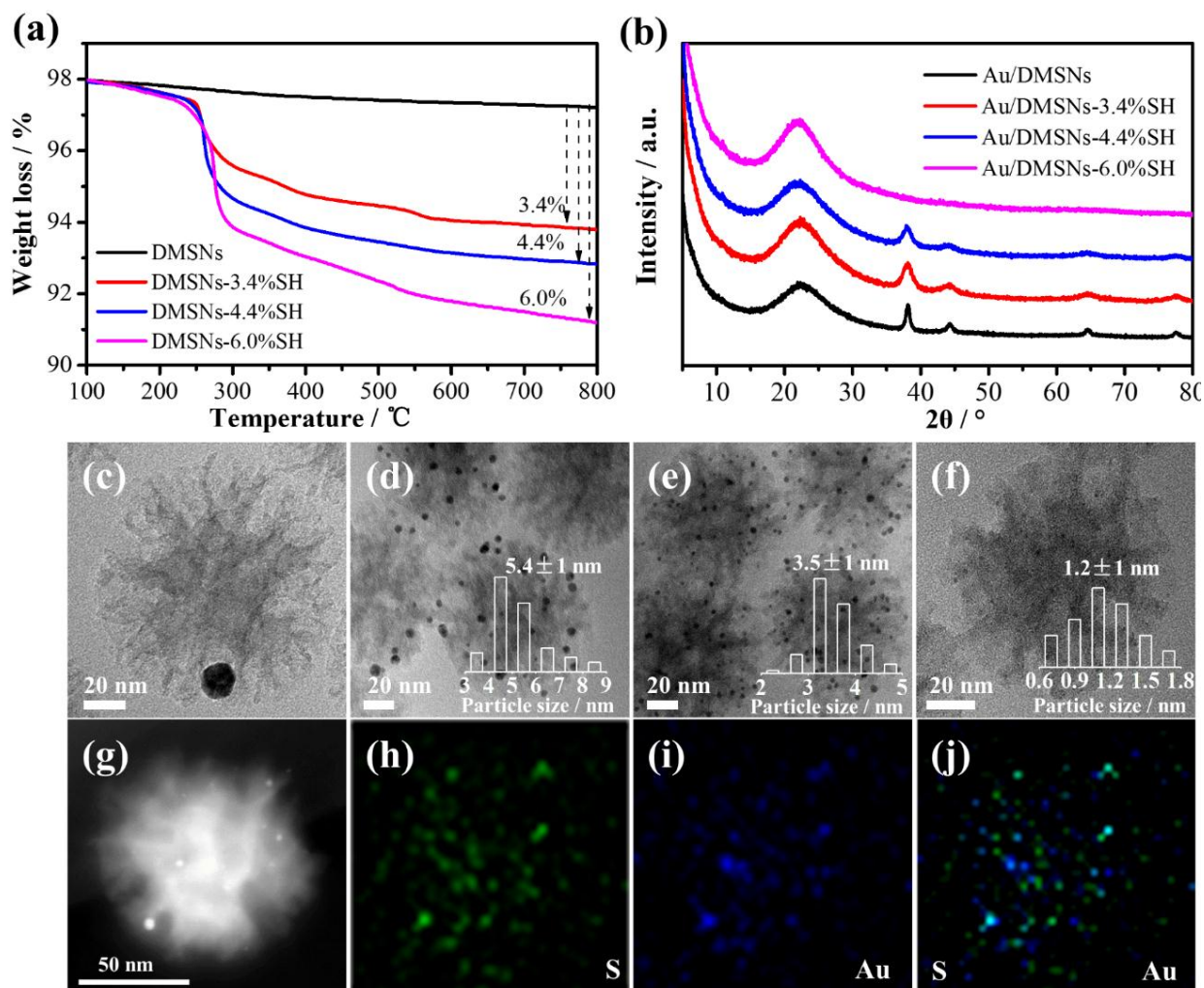


Figure 1. (a) Thermogravimetric curves of DMSNs-x%SH; (b) XRD patterns of Au/DMSNs-x%SH; (c-f) HRTEM images and AuNPs particle size distribution (c-f, insert) of Au/DMSNs-x%SH catalysts: (c) Au/DMSNs, (d) Au/DMSNs-3.4%SH (e) Au/DMSNs-4.4%SH and (f) Au/DMSNs-6.0%SH; High-resolution HAADF-STEM (g) of Au/DMSNs-4.4%SH and corresponding STEM-energy dispersive X-ray (EDX) elemental mapping images of S (h), Au (i) and S + Au composite (j) elements.

ligands as reference to non-modified DMSNs calculated in TG analysis (the weight loss from 200 °C to 500 °C was ascribed to the decomposition of organic moiety of MPTMS, Fig. 1a). Finally, Au NPs immobilized catalysts (Au/DMSNs-x%SH) were synthesized as such: gold

precursor (HAuCl_4) was firstly anchored by the thiol ligands on the silica wall and then reduced by NaBH_4 .²⁴⁻²⁶ Note that Au/DMSNs were prepared with the same method but using parent DMSNs as supports. The powder XRD patterns of Au NPs immobilized on the DMSNs clearly showed that the size of Au NPs was significantly decreased with the increase of thiol group loading (Fig. 1b). If without the introduction of thiol groups, a sharp peaks of Au/DMSNs catalyst at $2\theta = 38.2^\circ$ was observed (Fig. 1b, black line), which was assigned to the (111) planes of crystalline gold with larger size. However, in the presence of thiol groups, the XRD patterns of Au/DMSNs-x%SH showed a wide diffraction peak and with the increase of thiol loading from 3.4% to 4.4%, the full width at half maximum (FWHM) of the peak at $2\theta = 38.1^\circ$ became broader (Fig. 1b, red and blue line), suggesting the formation of Au NPs with smaller sizes. If further raising the content of thiol groups to 6.0%, the feature peaks of crystalline Au completely disappeared, indicating the formation of Au nanoclusters (NCs) with size less than 2.0 nm²⁷. Obviously, the formation of Au NPs and/or NCs is attributed to the strong binding interaction between gold and thiol ligands (S-Au) and its packing density on the Au core, which limits further growth of Au nucleus. The size evolution of Au NPs with the loading of thiol groups was further confirmed by HRTEM observation (Fig. 1c-f): highly dispersed Au NPs with average diameter of 5.4 nm, 3.5 nm and 1.2 nm were uniformly loaded on the surface of DMSNs support for Au/DMSNs-3.4%SH, Au/DMSNs-4.4%SH and Au/DMSNs-6.0%SH, respectively; Whereas, crystalline Au NPs in a size of ~19 nm was observed on parent DMSNs. In addition, STEM energy dispersive X-ray (EDX) mapping images (Fig. 1g-j) of Au/DMSNs-4.4%SH as a typical example suggested that both S and Au elements were homogeneously distributed onto the dendritic nanopores, implying that the thiol ligands played a key role to control the high dispersibility and the final particles size of Au NPs in the dendritic pores, which answers the

origin of volcano-type catalytic performance dependent on the size of Au NPs for selective oxidation of benzyl alcohol (Fig. 2a).

Gas-phase oxidation of benzyl alcohol over Au/DMSNs and Au/DMSNs-*x*%SH catalysts were performed at fixed-bed reactor at 250 °C. Generally, Au based catalysts showed high selectivity in the conversion of benzyl alcohol to benzaldehyde as observed in our Au/DMSNs catalysts (*sel.* > 95%, Fig. 2a), and only trace amount of benzoic acid as by-products was detected owing to the over-oxidation of benzaldehyde at high reaction temperature.¹ Thus, we

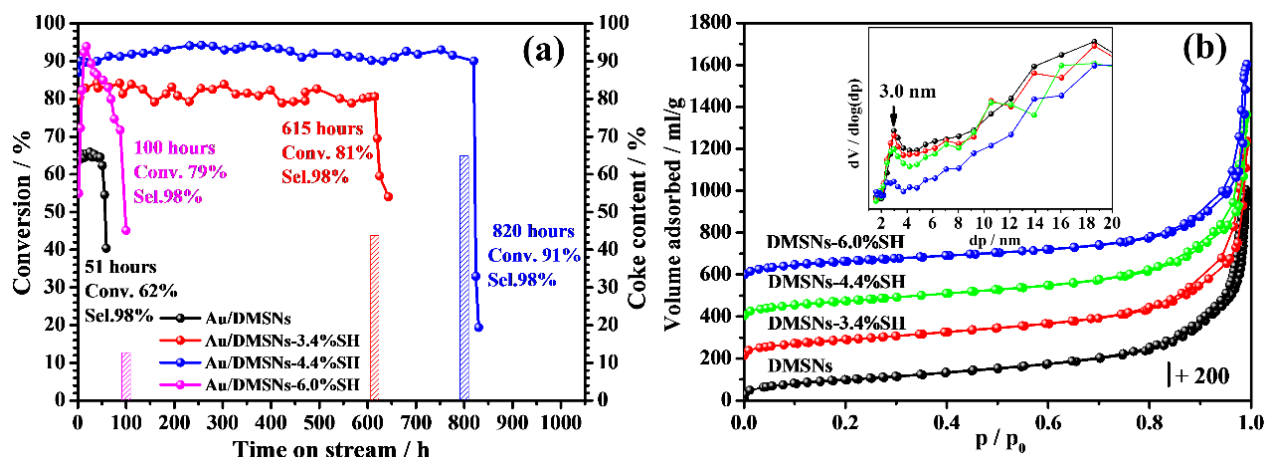


Figure 2. (a) Time-on-stream benzyl alcohol conversion (dot-lines) and coke contents (histogram) over Au/DMSNs-*x*%SH catalysts. (b) N₂ adsorption-desorption isotherms and pore size distribution (insert) plots of Au/DMSNs-*x*%SH.

mainly focus on the discussion of metal particle size effect on the chemical activity and stability of Au based catalyst on the reaction. As expectedly, due to the chemical inertness of bulky Au, Au/DMSNs with the largest Au particle size (~19 nm) showed the lowest conversion (~ 62%) and the shortest lifetime (only 51 hours) in the Fig. 2a. Very interestingly, the activity and lifetime gradually increased with the decrease of Au particle size (the conversion are 81% and

91%, and lifetimes are 615 hours and 820 hours for Au/DMSNs-3.4%SH with the size of 5.4 nm and Au/DMSNs-4.4%SH with size of 3.5 nm, respectively), whereas, a further decrease in size of Au NPs resulted in a decrease in the activity with an initial conversion of 54% and lifetime (100 hours) for Au/DMSNs-6.0%SH with the size of 1.2 nm. This size-dependent volcano-type trend was also observed for Au based catalysts in catalytic oxidation of carbon monoxide²⁸⁻³⁰ and liquid-phase oxidation of alcohol^{31, 32}. Generally, according to the quantum confinement effect, smaller sized Au exhibits better catalytic performance due to the favorite generation of superoxo-like species via electron transfer to the LUMO of the O₂ molecule³³⁻³⁷. XPS spectrum of Au 4f for Au/DMSNs-x%SH catalysts confirmed this point in the Figure 3: with the decrease of Au particle size, the Au 4f_{7/2} binding energy of Au/DMSNs-3.4%SH (5.4 nm), Au/DMSNs-4.4%SH (3.4 nm) and Au/DMSNs-6.0%SH (1.2 nm) was gradually shifted to low values in an order of 84.3 eV, 83.6 eV and 83.4 eV, indicating that small particle size of Au benefit the activation of oxygen molecules due to the substantial electron transfer from thiol ligands to Au core^{31, 38}. However, the size-dependent volcano-type trend verifies that it is not the case. It is possible that,

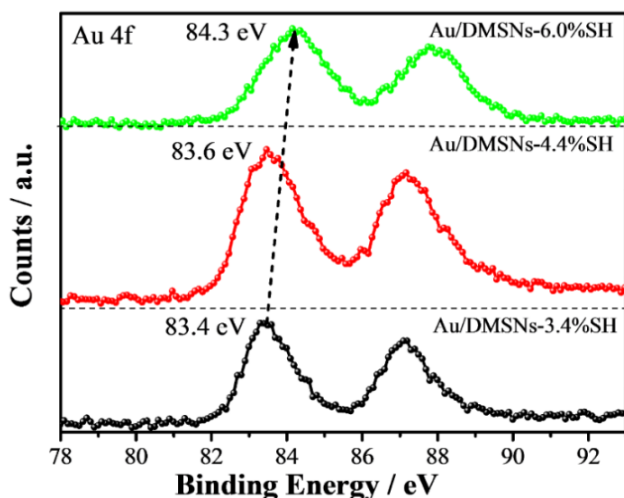


Figure 3. XPS spectrum of Au 4f (b) of Au/DMSNs-x%SH catalysts.

dense packing of thiol groups on the smaller Au core (1.2 nm) prohibits the adsorption of substrates, resulting in low chemical reactivity of Au/DMSNs-6.0%SH (Fig. 2a). This consideration can also interpret the time-on-stream activity change of Au/DMSNs-6.0%SH (firstly increased and then decreased, Fig. 2a, pink line), which denoted the grain growth of Au NPs at successive high-temperature reaction. Besides the difference in activity, similar to the Au core size control of thiol ligands, proper amount of thiol ligands can stabilize Au NPs against sintering, which dramatically increased the stability of the catalysts. With the increase in the content of thiol ligands, the lifetime of the catalysts dramatically increased from 50 h (Au/DMSNs) to 615 h (Au/DMSNs-3.4%SH) and to 820 h (Au/DMSNs-4.4%SH), it is worth noting that Au/DMSNs-4.4%SH with low loading of Au (~2%) achieved high benzaldehyde yield (*conv.* 91%, *sel.* 98%) and excellent catalytic stability for almost 820 h at 250 °C, which surpassed most of reported Au based catalysts^{1-10, 12, 13, 15, 17}. Whereas, in contrast, Au/DMSNs-6.0%SH suffered rapid deactivation in 100 h, which could be ascribed to the formation of substantial carbon deposition on the catalyst. The content of coke on the spent catalysts was positively correlated to the content of thiol ligands for catalysts (Fig. 2a and Fig. S1). For this regard, excess amount of thiol ligands grafted on DMSNs could block the pore network, which largely inhibited the mass diffusion of substrates and products. Fig. 2b shows the nitrogen sorption isotherm of DMSNs and DMSNs-x%SH, all the samples exhibit a typical IV isotherm with a hysteresis loop in the relative pressure range of 0.2-0.8, being characteristic of mesoporous materials, and have bimodal pore size distributions (Fig. 2b insert) in which small spherical mesopores with a micelle size (*ca.* 3.0 nm) nested in the dendritic channels (>10 nm)³⁹⁻⁴¹. Whereas, the absorbed volume of N₂ in this range decreased with the increase in the content of thiol ligands, suggesting the loss of specific surface area and pore volume of DMSNs after

grafting MPTMS. Detailed textural characteristics were shown in Table S1. Furthermore, almost all the specific surface area (97%) and pore volume of Au/DMSNs-6.0%SH was lost after reaction due to the fast coke deposition in the pores (Fig. S2b). While, both Au/DMSNs-3.4%SH and Au/DMSNs-4.4%SH samples showed the distinguished pore surface area and pore volume after the reaction (Fig. S2a and Table S1). Thus, the dramatically increased lifetime is the consequence of the strong stabilization of active gold nanoparticles by thiol ligand and the effective mass diffusion of DMSNs with unique opened three-dimensional mesoporous networks.

A very simple reaction mechanism on the benzyl alcohol oxidation by O₂ over Au NPs based catalysts was shown in Fig. 4. Owing to unique dendritic nanostructure of DMSNs and the strong S-Au binding energy at nanoscale interface, nanosized Au NPs were highly dispersed into the nanopores and could be acted as catalytic center for benzyl alcohol and oxygen adsorption (Fig. 4, in center). The adsorbed oxygen molecules were activated via electron transfer from Au NPs to the oxygen molecules (Step 1). The breaking of O-H bond of adsorbed benzyl alcohol can occur facilely with the aid of activated oxygen species to form Au-alkoxide intermediate and the C-H bond in the β position of benzyl alcohol was activated simultaneously (Step 2). Then, the oxido-intermediate can assist the cleavage of C-H bond in the β position and finally lead to the formation of benzaldehyde and water molecules, and concurrently an adsorbed O atom (O*) was formed on the Au core due to the O-O bond cleavage (Step 3), which could be active site to abstract the H atom from the OH group of the second benzyl alcohol molecule and formed an adsorbed hydroxyl group (Step 4). In the step 5, due to the strong p orbital interaction between hydroxyl and S atom from thiol groups (and/or adsorbed O atoms from the metal-alkoxide intermediate) via space interaction, a new formed p band transient intermediate state could be used as alternative channel to assist the cleavage of C-H bond in the β position of the second

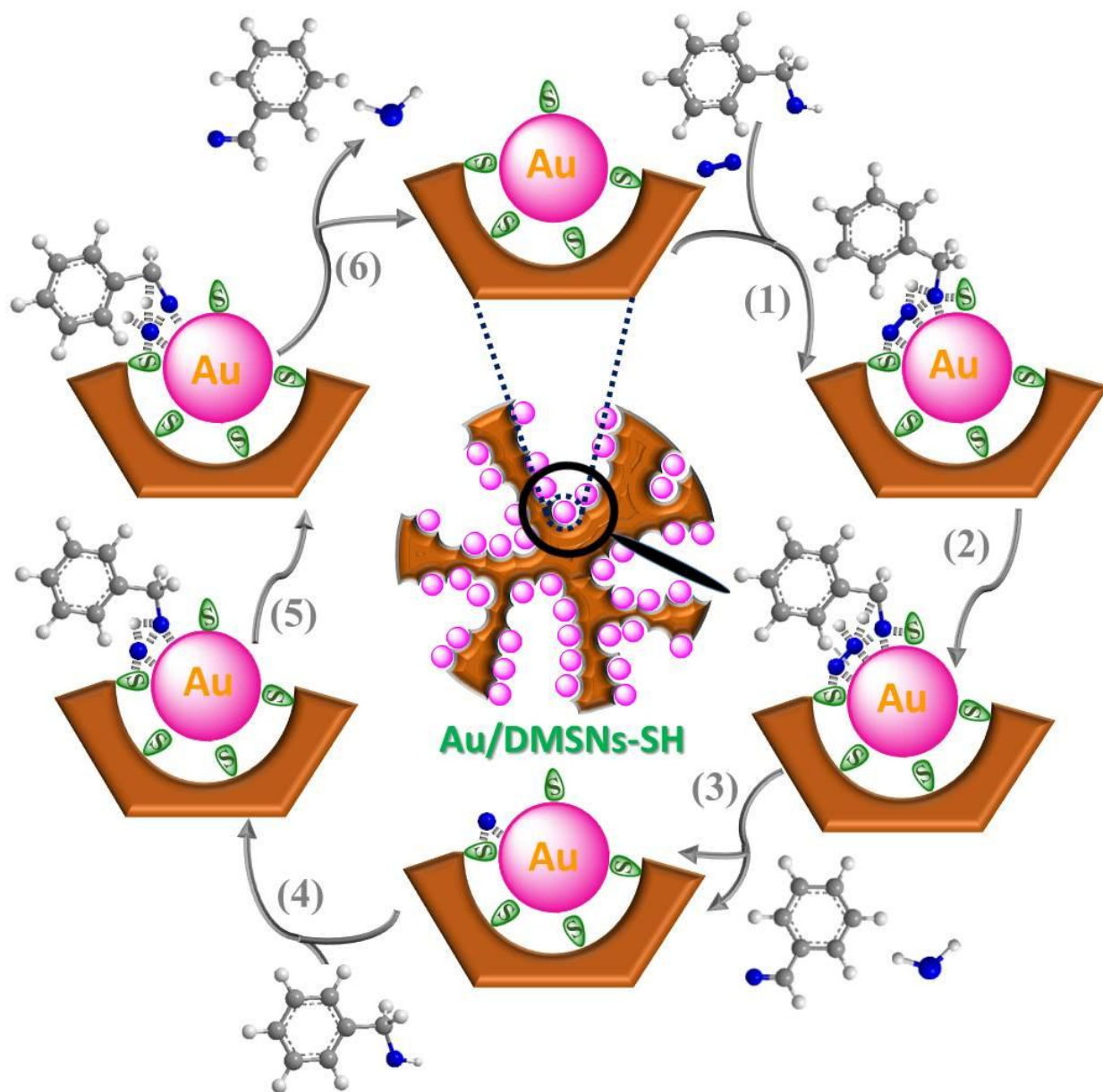


Figure 4. The proposed reaction scheme for gas-phase oxidation of benzyl alcohol by O_2 over Au based dendritic mesoporous silica nanospheres with thiol functional groups (Au/DMSNs-SH). For clarity, propyl segments were omitted.

benzyl alcohol molecule,⁴²⁻⁴⁸ and finally finished the catalytic cycle for the oxidation (Step 6). Obviously, the binding of thiol groups on Au core plays the pivotal role to control the

dispersibility of Au NPs in DMSNs, and the packing density of S-Au bonds determines the final chemical reactivity. Additionally, the strong interaction of p orbitals between adsorbed interfacial atoms from the surface ligands and substrates could weaken the chemisorption strength of Au-alkoxide intermediate, which avoids the over-oxidation of benzaldehyde and deposition of cokes, and consequently extending the lifetime of Au based catalysts.

3. CONCLUSIONS

In summary, Au NPs supported DMSNs catalysts functionalized with thiol groups in proper content were readily prepared by introducing propylamine as a base catalyst to improve the grafting efficiency of organosilane. We demonstrated that surface modified thiol groups played the key role in the catalytic performance of supported Au NPs catalysts in the gas-phase selective oxidation of benzyl alcohol, and that the introduction of proper content of thiol groups could improve the catalytic performance of the gas-phase selective oxidation of benzyl alcohol with high conversion (91%), high benzaldehyde selectivity (98%) and unprecedented long lifetime (*ca.* 820 h). Our finding paves the way for constructions of sintering- and coking-resistant active metal nanocatalysts and may open up the possibilities of transferring nanoscale metal catalysts from the laboratory to industry.⁴⁹⁻⁵¹

4. AUTHOR INFORMATION

Author Contributions

LXZ and BP equally contribute to this research. KZ conceived and directed the project. KZ, LXZ and BP co-designed the figures and wrote the manuscript with the help of QSX. All authors have read and agreed to the published version of the manuscript.

Notes

The authors declare no competing financial interest.

5. ACKNOWLEDGMENTS

This research was funded by the NSFC (22172051, 21872053 and 21573074), the Science and Technology Commission of Shanghai Municipality (19520711400), the Open Project Program of Academician and Expert Workstation, Shanghai Curui Low-Carbon Energy Technology Co., Ltd., and the JORISS program. K.Z. thanks ENS de Lyon for a temporary position as an invited professor in France.

6. REFERENCES

1. Fan, J., et al., Low-Temperature, Highly Selective, Gas-Phase Oxidation of Benzyl Alcohol over Mesoporous K-Cu-TiO₂ with Stable Copper(I) Oxidation State. *J. Am. Chem. Soc.*, 2009. 131: p. 15568–15569.
2. Zhan, G., et al., Bimetallic Au–Pd/MgO as efficient catalysts for aerobic oxidation of benzyl alcohol: A green bio-reducing preparation method. *Appl. Catal. A Gen.*, 2012. 439-440: p. 179-186.
3. Dai, Y., et al., Selectivity switching resulting in the formation of benzene by surface carbonates on ceria in catalytic gas-phase oxidation of benzyl alcohol. *Chem. Commun.*, 2016. 52(13): p. 2827-2830.
4. Yu, Y., et al., Highly selective oxidation of benzyl alcohol to benzaldehyde with hydrogen peroxide by biphasic catalysis. *Chem. Eng. J.*, 2010. 162(2): p. 738-742.
5. Liu, L., et al., Bimetallic Gold-Silver Nanoparticles Supported on Zeolitic Imidazolate Framework-8 as Highly Active Heterogenous Catalysts for Selective Oxidation of Benzyl Alcohol into Benzaldehyde. *Polymers*, 2018. 10(10): p. 1089.

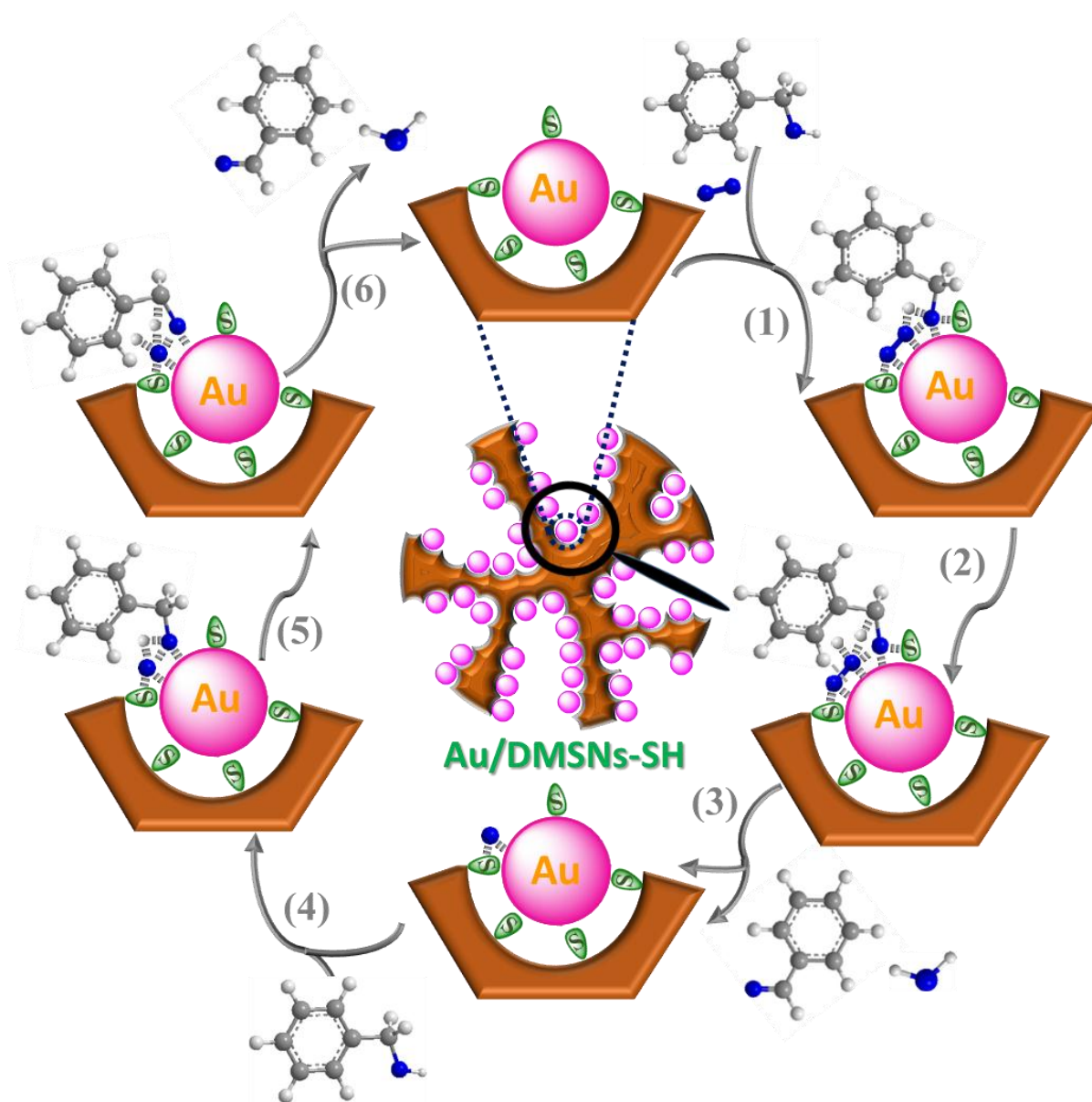
6. Della Pina, C., E. Falletta, and M. Rossi, Highly selective oxidation of benzyl alcohol to benzaldehyde catalyzed by bimetallic gold–copper catalyst. *J. Catal.*, 2008. 260(2): p. 384-386.
7. Yamamoto, R., et al., Promoted partial oxidation activity of supported Ag catalysts in the gas-phase catalytic oxidation of benzyl alcohol. *J. Catal.*, 2005. 234(2): p. 308-317.
8. Jia, L., et al., Highly selective gas-phase oxidation of benzyl alcohol to benzaldehyde over silver-containing hexagonal mesoporous silica. *Micropor. Mesopor. Mater.*, 2012. 149(1): p. 158-165.
9. Ma, L., et al., Catalytic activity of Ag/SBA-15 for low-temperature gas-phase selective oxidation of benzyl alcohol to benzaldehyde. *Chin. J. Catal.*, 2014. 35(1): p. 108-119.
10. Biella, S. and M. Rossi, Gas phase oxidation of alcohols to aldehydes or ketones catalysed by supported gold. *Chem. Commun.*, 2003(3): p. 378-9.
11. Zhao, G., et al., Microstructured Au/Ni-fiber catalyst for low-temperature gas-phase selective oxidation of alcohols. *Chem. Commun.*, 2011. 47(34): p. 9642-4.
12. Yi, W., et al., A Rational Solid-State Synthesis of Supported Au–Ni Bimetallic Nanoparticles with Enhanced Activity for Gas-Phase Selective Oxidation of Alcohols. *ACS Appl. Mater. Interfaces*, 2017. 9(37): p. 31853-31860.
13. Hayashibara, H., et al., The effect of alkali promoters on Cu-Na-ZSM-5 catalysts in the oxidation of benzyl alcohol. *J. Catal.*, 1995. 153: p. 254-264.
14. Zhao, G., et al., Metal/oxide interfacial effects on the selective oxidation of primary alcohols. *Nat. Commun.*, 2017. 8: p. 14039.
15. Liu, K., et al., Synergistic effect between Ag and Mn₃O₄ in the gas phase oxidation of alcohols. *Catal. Commun.*, 2018. 113: p. 15-18.

16. Li, T., et al., Maximizing the Number of Interfacial Sites in Single-Atom Catalysts for the Highly Selective, Solvent-Free Oxidation of Primary Alcohols. *Angew. Chem. Int. Ed.*, 2018. 57(26): p. 7795-7799.
17. Ma, G., et al., Ordered Nanoporous Silica with Periodic 30-60 nm Pores as an Effective Support for Gold Nanoparticle Catalysts with Enhanced Lifetime. *J. Am. Chem. Soc.*, 2010. 132: p. 9596-9597.
18. Zhang, K., et al., Dendritic and Core-Shell-Corona Mesoporous Sister Nanospheres from Polymer-Surfactant-Silica Self-Entanglement. *Chem. Eur. J.*, 2018. 24: p. 478–486.
19. Hao, P., et al., Comprehensive understanding of the synthesis and formation mechanism of dendritic mesoporous silica nanospheres. *Nanoscale Adv.*, 2020.
20. Du, X. and S.Z. Qiao, Dendritic silica particles with center-radial pore channels: promising platforms for catalysis and biomedical applications. *Small*, 2015. 11(4): p. 392-413.
21. Maity, A. and V. Polshettiwar, Dendritic Fibrous Nanosilica for Catalysis, Energy Harvesting, Carbon Dioxide Mitigation, Drug Delivery, and Sensing. *ChemSusChem*, 2017. 10(20): p. 3866-3913.
22. Peng, H., et al., Catalysts in Coronas: A Surface Spatial Confinement Strategy for High-Performance Catalysts in Methane Dry Reforming. *ACS Catal.*, 2019. 9(10): p. 9072-9080.
23. Wang, Y., et al., Dendritic fibrous nano-particles (DFNPs): rising stars of mesoporous materials. *J. Mater. Chem. A*, 2019. 7(10): p. 5111-5152.
24. Yang, T.-Q., et al., Interfacial electron transfer promotes photo-catalytic reduction of 4-nitrophenol by Au/Ag₂O nanoparticles confined in dendritic mesoporous silica nanospheres. *Catal. Sci. Technol.*, 2019. 9(20): p. 5786-5792.

25. Shan, B.Q., et al., One-pot co-condensation strategy for dendritic mesoporous organosilica nanospheres with fine size and morphology control. *CrystEngComm*, 2019. 21(27): p. 4030-4035.
26. Yu, Y.J., et al., Facile synthesis of size controllable dendritic mesoporous silica nanoparticles. *ACS Appl. Mater. Interfaces*, 2014. 6(24): p. 22655-65.
27. Yang, T.-Q., et al., Origin of the Photoluminescence of Metal Nanoclusters: From Metal-Centered Emission to Ligand-Centered Emission. *Nanomaterials*, 2020. 10(2): p. 261.
28. Haruta, M., et al., Gold Catalysts Prepared by Coprecipitation for Low-Temperature Oxidation of Hydrogen and of Carbon Monoxide. *J. Catal.*, 1989. 115: p. 301-309.
29. Haruta, M., Size- and support-dependency in the catalysis of gold. *Catal. Today*, 1997. 36: p. 153-166.
30. Valden, M., X. Lai, and D.W. Goodman, Onset of Catalytic Activity of Gold Clusters on Titania with the Appearance of Nonmetallic Properties. *Science*, 1998. 281: p. 1647-1650.
31. Tsunoyama, H., et al., Effect of Electronic Structures of Au Clusters Stabilized by Poly(N-vinyl-2-pyrrolidone) on Aerobic Oxidation Catalysis. *J. Am. Chem. Soc.*, 2009. 131: p. 7086-7093.
32. Tsunoyama, H., et al., Size-Specific Catalytic Activity of Polymer-Stabilized Gold Nanoclusters for Aerobic Alcohol Oxidation in Water. *J. Am. Chem. Soc.*, 2005. 127: p. 9374-9375.
33. Kim, Y.D., M. Fischer, and G. Ganteför, Origin of unusual catalytic activities of Au-based catalysts. *Chem. Phys. Lett.*, 2003. 377(1-2): p. 170-176.
34. Yoon, B., H. Häkkinen, and U. Landman, Interaction of O₂ with Gold Clusters: Molecular and Dissociative Adsorption. *J. Phys. Chem. A*, 2003. 107: p. 4066-4071.

35. Qiao, B., et al., Ultrastable single-atom gold catalysts with strong covalent metal-support interaction (CMSI). *Nano Res.*, 2015. 8(9): p. 2913-2924.
36. Qiao, B., et al., Highly Efficient Catalysis of Preferential Oxidation of CO in H₂-Rich Stream by Gold Single-Atom Catalysts. *ACS Catal.*, 2015. 5(11): p. 6249-6254.
37. Tang, Y., et al., On the Nature of Support Effects of Metal Dioxides MO₂ (M = Ti, Zr, Hf, Ce, Th) in Single-Atom Gold Catalysts: Importance of Quantum Primogenic Effect. *J. Phys. Chem. C*, 2016. 120(31): p. 17514-17526.
38. Negishi, Y., K. Nobusada, and T. Tsukuda, Glutathione-Protected Gold Clusters Revisited: Bridging the Gap between Gold(I)-Thiolate Complexes and Thiolate-Protected Gold Nanocrystals. *J. Am. Chem. Soc.*, 2005. 127: p. 5261-5270.
39. Zhang, K., et al., Facile large-scale synthesis of monodisperse mesoporous silica nanospheres with tunable pore structure. *J. Am. Chem. Soc.*, 2013. 135(7): p. 2427-30.
40. Liu, P.C., et al., A dual-templating strategy for the scale-up synthesis of dendritic mesoporous silica nanospheres. *Green Chem.*, 2017. 19(23): p. 5575-5581.
41. Peng, B., et al., Interfacial Charge Shielding Directs Synthesis of Dendritic Mesoporous Silica Nanospheres by a Dual-Templating Approach. *New J. Chem.*, 2019. 43: p. 15777-15784.
42. Yang, T., et al., P band intermediate state (PBIS) tailors photoluminescence emission at confined nanoscale interface. *Commun. Chem.*, 2019. 2(1): p. 1-11.
43. Hu, X.-D., et al., Interfacial Hydroxyl Promotes the Reduction of 4-Nitrophenol by Ag-based Catalysts Confined in Dendritic Mesoporous Silica Nanospheres. *J. Phys. Chem. C*, 2021. 125(4): p. 2446-2453.

44. Shan, B.Q., et al., Surface electronic states mediate concerted electron and proton transfer at metal nanoscale interfaces for catalytic hydride reduction of -NO₂ to -NH₂. *Phys. Chem. Chem. Phys.*, 2021. 23: p. 12950-12957.
45. Tao, R., et al., Surface Molecule Manipulated Pt/TiO₂ Catalysts for Selective Hydrogenation of Cinnamaldehyde. *J. Phys. Chem. C*, 2021. 125(24): p. 13304-13312.
46. Yang, T.-Q., et al., Caged structural water molecules emit tunable brighter colors by topological excitation. *Nanoscale*, 2021. 13(35): p. 15058-15066.
47. Zhou, J., et al., Structural Water Molecules Confined in Soft and Hard Nanocavities as Bright Color Emitters. *ACS Phys. Chem. Au*, 2021. <https://doi.org/10.1021/acspphyschemau.1c00020>.
48. Peng, B., et al., Physical Origin of Dual-Emission of Au–Ag Bimetallic Nanoclusters. *Front. Chem.*, 2021. 9: p. 756993.
49. Deng, Y., et al., Embedding Ultrasmall Au Clusters into the Pores of a Covalent Organic Framework for Enhanced Photostability and Photocatalytic Performance. *Angew. Chem. Int. Ed.*, 2020. 59(15): p. 6082-6089.
50. Sha, J., et al., Single-reactor tandem oxidation–amination process for the synthesis of furan diamines from 5-hydroxymethylfurfural. *Green Chem.*, 2021. 23(18): p. 7093-7099.
51. Wang, T., et al., Identification of active catalysts for the acceptorless dehydrogenation of alcohols to carbonyls. *Nat. Commun.*, 2021. 12(1)



High efficient and stable thiol-modified dendritic mesoporous silica nanospheres supported gold catalysts were facially synthesized by introducing propylamine as a base catalyst to improve the grafting efficiency of organosilanes, which exhibited high catalytic performance in high-temperature gas phase selective oxidation of benzyl alcohol with ultra-long lifetime up to 800 hours, beyond all the reported metal based catalysts.